Green One-Pot Synthesis of Imidazole Derivatives Using Fruit Peel Extracts as Natural Acid Catalysts: Characterization, Antimicrobial Activity and Preliminary Cu^{2+} Recognition Studies

Vaishnavi Bharat Deshmukh[1], Dr. Sangita Satpute[2]
[1] *Department of Chemistry, Vidya Pratishthan's Arts, Science and Commerce College, Baramati, Maharashtra 413133, India*
[2] *Associate Professor and PG Coordinator Department of Chemistry, Vidya Pratishthan's Arts, Science and Commerce College, Baramati, Maharashtra 413133, India*

Abstract*—A simple and environmentally benign one-pot method was developed for the synthesis of substituted imidazole derivatives using aqueous fruit peel extracts as natural acid catalysts. Lemon (*Citrus limon*), orange (*Citrus sinensis*) and pomegranate (*Punica granatum*) peel extracts were prepared in water and evaluated as catalysts for the condensation of benzil, aromatic aldehydes and ammonium acetate. Two representative imidazole derivatives were synthesized using cinnamaldehyde and anisaldehyde as aldehyde components. The catalytic performance of the fruit peel extracts was compared with catalyst-free and ethanol-mediated reaction conditions. Under solvent-free conditions, lemon peel extract gave the highest isolated yields of 55.58% for the cinnamaldehyde-derived product and 50.79% for the anisaldehyde-derived product within 45 min. The synthesized products were characterized by thin-layer chromatography, melting-point determination, UV–Visible spectroscopy, FTIR spectroscopy, ^{1}H NMR and ^{13}C NMR spectroscopy. The spectroscopic data supported formation of the imidazole framework. Preliminary antibacterial evaluation against *Staphylococcus aureus* showed measurable inhibition for the products prepared using lemon peel extract. Interaction of the synthesized compounds with Cu^{2+} ions was further investigated by UV–Visible spectroscopy and cyclic voltammetry, with observable changes in absorption intensity and electrochemical response following Cu^{2+} addition. The results demonstrate the potential of fruit peel extracts as inexpensive and renewable catalysts for imidazole synthesis and provide preliminary evidence for Cu^{2+} recognition by the synthesized heterocyclic compounds.

***Index Terms*—Green synthesis; imidazole derivatives; fruit peel extract; natural catalyst; one-pot synthesis, antimicrobial activity; Cu^{2+} recognition.**

Highlights

- A simple one-pot synthesis of imidazole derivatives was developed using fruit peel extracts.
- Lemon, orange and pomegranate peel extracts were evaluated as renewable natural catalysts.
- Lemon peel extract gave the highest yields under solvent-free conditions.
- The synthesized compounds were characterized by UV–Visible, FTIR, ^{1}H NMR and ^{13}C NMR spectroscopy.
- The synthesized compounds showed preliminary antibacterial activity.
- UV–Visible and cyclic-voltammetric studies indicated interaction with Cu^{2+} ions.
- The method demonstrates a potential approach for valorization of fruit peel waste in green organic synthesis.

I. INTRODUCTION

Imidazole is an important nitrogen-containing heterocyclic framework that occurs in several biologically relevant molecules and serves as a useful structural unit in medicinal, coordination and materials chemistry. Substituted imidazole derivatives have attracted considerable attention

because of their diverse biological and chemical properties. The imidazole nitrogen atoms can also participate in coordination with metal ions, making imidazole-containing compounds useful candidates for molecular recognition and sensing studies. The classical synthesis of substituted imidazoles commonly involves the condensation of a 1,2-dicarbonyl compound, an aldehyde and an ammonia or ammonium source, as represented by the Debus–Radziszewski reaction. Although conventional synthetic procedures are effective, they may involve corrosive acid catalysts, organic solvents, elevated temperatures and relatively long reaction times. These limitations have encouraged the development of greener synthetic approaches. [5,6]

Green chemistry aims to reduce the use and generation of hazardous substances while improving the efficiency and sustainability of chemical processes. In this context, agricultural and food-processing wastes are attractive renewable resources because they are inexpensive, readily available and contain several naturally occurring organic compounds. Fruit peels, in particular, contain organic acids and other phytochemicals that can provide acidic catalytic environments. Their direct use as catalysts also provides an opportunity for waste valorization. One-pot multicomponent reactions are particularly attractive from a green chemistry perspective because several reactants can be converted into the desired product in a single reaction vessel. Such procedures can reduce the number of isolation and purification steps, decrease solvent consumption and simplify the overall synthetic process. [10,11]

The present study therefore investigates a simple one-pot synthesis of substituted imidazole derivatives using aqueous extracts of lemon, orange and pomegranate peels as natural acid catalysts. The catalytic efficiency of the extracts was compared under different reaction conditions. The synthesized compounds were characterized using TLC, melting-point determination, UV–Visible spectroscopy, FTIR, ^{1}H NMR and ^{13}C NMR spectroscopy. Their preliminary antibacterial activity and interaction with Cu^{2+} ions were also examined. The principal objective was to establish a simple, inexpensive and environmentally preferable route for the preparation of imidazole derivatives using fruit peel waste as a renewable catalytic material. [10,12,13]

II. MATERIALS AND METHODS

2.1 Chemicals and reagents

Benzil, substituted aromatic aldehydes, ammonium acetate, ethanol, methanol, ethyl acetate, hexane, dimethyl sulfoxide (DMSO), copper(II) sulfate pentahydrate ($CuSO_4 \cdot 5H_2O$) and potassium bromide (KBr) were obtained from commercial sources and used without further purification. Deionized water was used for preparation of aqueous solutions and fruit peel extracts. Fresh lemon, orange and pomegranate fruits were obtained from the local market. The corresponding peels were used for preparation of the natural catalysts.

2.2 Instrumentation

The synthesized compounds were characterized by UV–Visible spectroscopy, FTIR spectroscopy, ^{1}H NMR spectroscopy and ^{13}C NMR spectroscopy. TLC was used to monitor the reaction and assess the preliminary purity of the products. Melting points were determined using a digital melting-point apparatus. UV–Visible measurements were also used to investigate changes associated with interaction between the synthesized compounds and Cu^{2+} ions. Cyclic voltammetry was performed using an electrochemical workstation equipped with a three-electrode configuration. [3,4]

2.3 Preparation of fruit peel extracts

Fresh lemon, orange and pomegranate peels were thoroughly washed with deionized water to remove surface contaminants. The peels were shade-dried and subsequently ground to obtain a fine powder. For each extract, 10 g of dried peel powder was suspended in 100 mL of deionized water. The suspension was heated at 80–90 °C for 15 min with continuous stirring. After cooling to room temperature, the mixture was filtered through Whatman No. 1 filter paper. The resulting aqueous extracts were stored at 4 °C until use as natural catalysts.

2.4 Green one-pot synthesis of imidazole derivatives

The imidazole derivatives were synthesized through a one-pot multicomponent condensation of benzil, an aromatic aldehyde and ammonium acetate. In a typical reaction, benzil (1 mmol, 0.21 g), the selected aldehyde (1 mmol) and ammonium acetate (2 mmol,

0.154 g) were mixed with 0.5–1.0 mL of the prepared fruit peel extract. The reaction mixture was heated at 80–100 °C under continuous stirring. The reaction progress was monitored by TLC. After completion, the reaction mixture was allowed to cool to room temperature. The precipitated solid was collected by filtration and washed with chilled deionized water. The crude product was dried and purified by recrystallization from hot ethanol.

Two representative derivatives were prepared:

Compound 1: benzil + cinnamaldehyde + ammonium acetate → 2-styryl-4,5-diphenylimidazole.

Compound 2: benzil + anisaldehyde + ammonium acetate → 2-(4-methoxyphenyl)-4,5-diphenylimidazole.

2.5 Reaction optimization and characterization of synthesized compounds

The synthesized imidazole derivatives were evaluated under three different reaction conditions to determine the influence of the catalyst and reaction medium on the reaction efficiency. In Method A, the reaction was performed under catalyst-free and solvent-free conditions, whereas Method B employed the respective fruit peel extract as a natural catalyst under solvent-free conditions. In Method C, the fruit peel extract was used as a catalyst in ethanol under reflux conditions. The reactions were monitored by thin-layer chromatography (TLC), and the reaction time, isolated yield, melting point and chromatographic behavior of the products were compared to determine the most favorable reaction conditions.

The isolated products were purified and characterized by melting-point determination and spectroscopic techniques. Melting points were determined using a digital melting-point apparatus by placing the dried samples in sealed capillary tubes and recording the temperature range over which the solid melted. TLC analysis was performed on pre-coated silica gel plates using ethyl acetate–hexane as the mobile phase, and the developed chromatograms were visualized under UV light. The retention factor (Rf) was calculated as the ratio of the distance travelled by the compound to that travelled by the solvent front.

The electronic absorption characteristics of the synthesized compounds were investigated using UV–Visible spectroscopy in the wavelength range of 200–800 nm. FTIR spectra were recorded in the range of 4000–400 cm^{-1} using the KBr pellet technique to identify the characteristic functional groups associated with the synthesized imidazole derivatives. The compounds were further characterized by ^{1}H and ^{13}C NMR spectroscopy. The NMR spectra were recorded using appropriate deuterated solvents, and chemical shifts were reported in ppm relative to the internal reference. The spectral data were interpreted based on the characteristic signals corresponding to the aromatic and imidazole moieties and other substituents present in the synthesized compounds. [14,15]

2.6 Antibacterial activity

The antibacterial activity of the synthesized compounds was evaluated using the agar well/diffusion method. The test compounds were evaluated at a concentration of 50 µg per disc/well according to the experimental procedure used in the study. The bacterial culture was spread uniformly over sterile nutrient agar plates. Wells/discs containing the test compounds were applied to the inoculated plates. Ciprofloxacin and gentamicin were used as reference antibiotics, while DMSO served as the negative control. The plates were incubated at 37 °C for 24 h, after which the inhibition zones were measured in millimetres.

Cu^{2+} interaction studies by UV–Visible spectroscopy and cyclic voltammetry

The interaction of the synthesized imidazole derivatives with Cu^{2+} ions was investigated using UV–Visible spectroscopy and cyclic voltammetry. For the spectrophotometric study, a solution of the synthesized imidazole derivative was treated with increasing concentrations of $CuSO_4$ solution prepared in phosphate buffer at pH 7.0. The UV–Visible spectra were recorded after the addition of Cu^{2+}, and changes in absorption intensity and spectral features were monitored to evaluate the interaction between the imidazole derivative and Cu^{2+} ions.

The electrochemical behavior of the synthesized imidazole derivative in the presence of Cu^{2+} was further investigated by cyclic voltammetry using a conventional three-electrode system consisting of a glassy carbon working electrode, platinum wire counter electrode and Ag/AgCl reference electrode. Measurements were performed in phosphate buffer at pH 7.0 over a potential range of −0.2 to +0.8 V at a scan rate of 50 mV s^{-1}. The electrochemical response

was recorded before and after the addition of $CuSO_4$, and the resulting changes in peak current and peak potential were analyzed to assess the interaction of the synthesized imidazole derivative with Cu^{2+} ions.

III. RESULTS AND DISCUSSION

3.1 Optimization of reaction conditions

The synthesis of the imidazole derivatives was evaluated under three reaction conditions to investigate the influence of the fruit peel extract and reaction medium on the reaction efficiency. The results obtained for the cinnamaldehyde- and anisaldehyde-derived products are summarized in Tables 1 and 2, respectively. For the cinnamaldehyde-derived derivative, the catalyst-free and solvent-free reaction (Method A) afforded a 40.55% yield after 60 min. The introduction of fruit peel extracts under solvent-free conditions (Method B) improved both the reaction yield and reaction time. Among the three extracts investigated, lemon peel extract afforded the highest yield of 55.58% in 45 min, followed by pomegranate peel extract (52.41%) and orange peel extract (50.98%). Thus, incorporation of the fruit peel extracts resulted in an increase in yield of approximately 10–15 percentage points compared with the catalyst-free reaction. A similar trend was observed for the anisaldehyde-derived derivative. The catalyst-free reaction afforded a yield of only 22.81% after 60 min, whereas the use of fruit peel extracts under solvent-free conditions increased the yield. Lemon peel extract again showed the highest catalytic activity, giving a yield of 50.79% after 45 min, while pomegranate and orange peel extracts afforded yields of 31.03% and 25.45%, respectively. The superior performance of the lemon peel extract may be related to the acidic and other phytochemical constituents naturally present in the extract. However, since the individual components of the extracts were not chemically characterized in the present study, a specific component cannot be identified as responsible for the observed catalytic activity.

The ethanol-mediated reactions (Method C) did not provide an improvement over the solvent-free fruit peel extract-catalyzed procedure. For the cinnamaldehyde-derived derivative, the yields obtained under Method C ranged from 17.69 to 39.35%, whereas the corresponding reactions for the anisaldehyde-derived derivative afforded yields of 12.26–16.31% with the fruit peel extracts. In addition, Method C required a longer reaction time of 90 min. These results indicate that, under the conditions investigated, the fruit peel extract-catalyzed solvent-free method (Method B) was more favorable than the ethanol-mediated procedure. Overall, lemon peel extract under solvent-free conditions was identified as the optimum condition among the methods investigated, providing the highest yields for both synthesized derivatives within the shorter reaction time of 45 min. The catalytic effect was therefore selected for subsequent synthesis and characterization studies.

Table 1. Effect of reaction conditions on the synthesis of the cinnamaldehyde-derived imidazole derivative

Method	Catalyst	Time (min)	Yield (%)	Melting point (°C)	*R*f
A	None	60	40.55	272	0.80
B	Orange peel extract	45	50.98	268	0.90
B	Lemon peel extract	45	55.58	271	0.90
B	Pomegranate peel extract	45	52.41	269	0.78
C	None	90	25.52	266	0.72
C	Orange peel extract	90	39.35	270	0.84
C	Lemon peel extract	90	36.70	269	0.74
C	Pomegranate peel extract	90	17.69	265	0.80

Table 2. Effect of reaction conditions on the synthesis of the anisaldehyde-derived imidazole derivative

Method	Catalyst	Time (min)	Yield (%)	Melting point (°C)	*R*f
A	None	60	22.81	271	0.90
B	Orange peel extract	45	25.45	269	0.85

B	Lemon peel extract	45	50.79	270	0.88
B	Pomegranate peel extract	45	31.03	272	0.90
C	None	90	24.84	268	0.82
C	Orange peel extract	90	16.31	272	0.78
C	Lemon peel extract	90	12.94	270	0.83
C	Pomegranate peel extract	90	12.26	265	0.76

3.2 Preliminary characterization by TLC and melting-point determination

The synthesized products were initially evaluated by TLC and melting-point determination. TLC analysis showed distinct spots for the isolated products, with *R*f values ranging from 0.72 to 0.90 for the cinnamaldehyde-derived series and from 0.76 to 0.90 for the anisaldehyde-derived series. The lemon peel extract-catalyzed products showed *R*f values of 0.90 and 0.88 for the cinnamaldehyde- and anisaldehyde-derived derivatives, respectively. The formation of distinct product spots and the disappearance of the corresponding starting-material spots during reaction monitoring supported the conversion of the starting materials.

The isolated products exhibited melting points in the range of 265–272 °C. For the optimized lemon peel extract-catalyzed reactions, the cinnamaldehyde-derived derivative showed a melting point of **271 °C**, whereas the anisaldehyde-derived derivative showed a melting point of **270 °C**. The observed melting points were consistent with the formation of relatively homogeneous crystalline products. However, TLC and melting-point measurements were considered preliminary characterization techniques, and structural confirmation was subsequently performed using UV–Visible, FTIR and NMR spectroscopy.

3.4 UV–Visible Spectroscopic Characterization

The UV–Visible absorption spectra of the synthesized compounds exhibited characteristic absorption bands in the ultraviolet region, confirming the presence of conjugated aromatic and heterocyclic chromophores. The major absorption bands were observed predominantly in the 200–230 nm region, which may be attributed to allowed π→π* electronic transitions associated with the aromatic and conjugated systems. Additional weaker absorptions at relatively longer wavelengths may be assigned to n→π* transitions involving heteroatoms present in the imidazole framework. Among the synthesized derivatives, the cinnamaldehyde-derived compound exhibited spectral characteristics indicative of an extended conjugated styryl system. The presence of this additional conjugation is expected to influence the electronic absorption profile and produce a relatively broader or shifted absorption compared with less extensively conjugated derivatives. Overall, the UV–Visible spectral features, in combination with the FTIR and NMR data, support the formation of the proposed conjugated imidazole derivatives. [14,15]

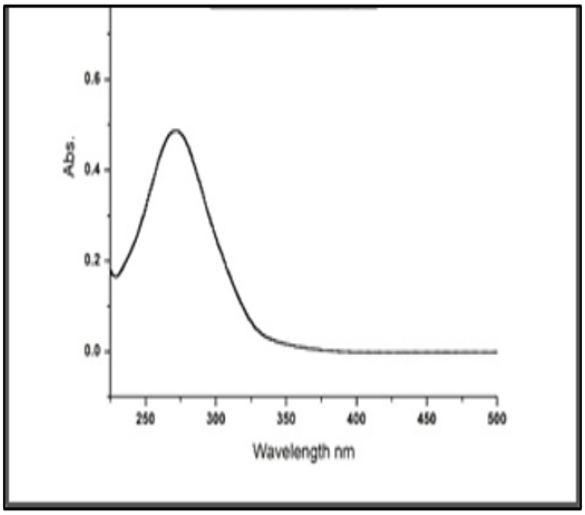

Figure 1. UV–Visible spectra of the synthesized imidazole derivatives obtained under different reaction conditions.

3.5 FTIR Spectroscopic Characterization

FTIR spectroscopy was employed to identify the characteristic functional groups present in the synthesized imidazole derivatives and to provide evidence for the proposed structural transformation. The FTIR spectra exhibited characteristic absorption bands corresponding to N–H stretching, C=N stretching, aromatic C=C vibrations, and C–N stretching vibrations.The disappearance or significant attenuation of the characteristic carbonyl absorption bands of the starting carbonyl compounds, accompanied by the appearance of bands

characteristic of the imidazole ring, indicates the conversion of the starting materials through condensation and subsequent cyclization. The observed spectral changes are therefore consistent with the formation of the desired imidazole derivatives. [14,15]

Table 3. Principal FTIR spectral assignments of the synthesized imidazole derivatives

Approximate wavenumber (cm^{-1})	Assignment
3100–3400	N–H stretching
1550–1665	C=N stretching
1450–1600	Aromatic C=C vibrations
1200–1350	C–N stretching

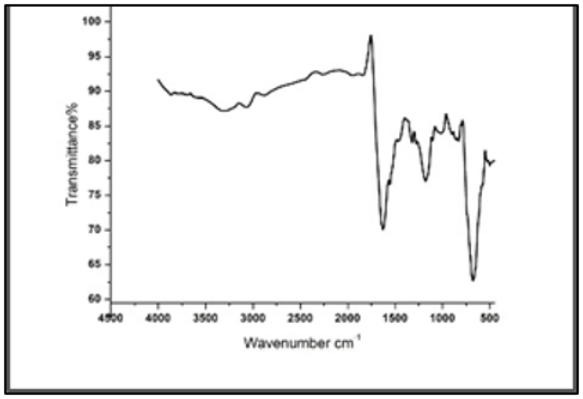

Figure 2. FTIR spectra of the synthesized imidazole derivatives.

The above assignments represent the characteristic spectral regions associated with the proposed functional groups. The individual experimental peak positions should be reported for each synthesized compound in the final manuscript to provide compound-specific structural confirmation.

3.6 ^{1}H NMR Characterization

The ^{1}H NMR spectra provided further structural evidence for the formation of the substituted imidazole derivatives. The observed resonances were predominantly located in the aromatic and heteroaromatic regions. Signals were generally observed within the δ 7.0–8.1 ppm range. A relatively downfield resonance near δ 8.0 ppm was assigned to the proton associated with the imidazole environment, whereas the signals in the δ 7.4–7.6 ppm region were attributed to aromatic protons of the substituted phenyl rings. A broad resonance appearing approximately in the δ 7.1–7.3 ppm region was assigned to the N–H proton. The overall chemical-shift distribution is consistent with the presence of the proposed substituted imidazole and aromatic moieties. The ^{1}H NMR observations, together with the FTIR and UV–Visible spectral data, support the proposed structures of the synthesized compounds. For definitive structural characterization, the complete experimental chemical shifts, multiplicities, coupling constants, and proton integrations should be reported for each individual derivative. [16,17,18,19]

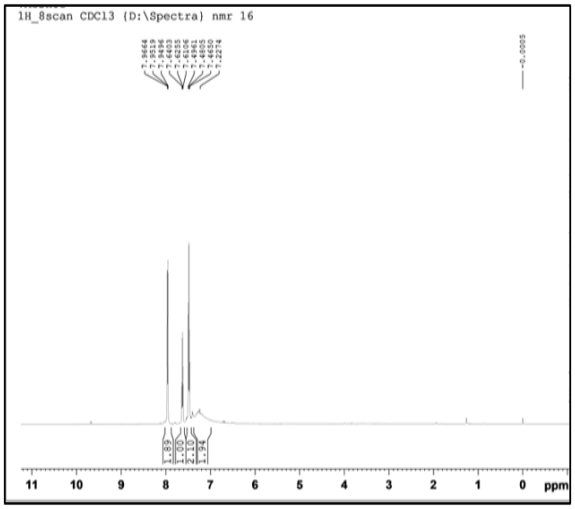

Figure 3. ^{1}H NMR spectrum of the synthesized imidazole derivative

3.7 ^{13}C NMR Characterization

The ^{13}C NMR spectra provided additional evidence for the formation of the proposed imidazole frameworks. The observed resonances were predominantly distributed in the aromatic and heteroaromatic carbon regions. A resonance at approximately δ 135 ppm was attributed to an imidazole carbon associated with the nitrogen-containing heterocyclic framework, while signals in the δ 129–133 ppm region were assigned primarily to aromatic carbon atoms. The absence of prominent resonances characteristic of the carbonyl carbons of the starting aldehyde/ketone components further supports their conversion during the condensation and cyclization process. The ^{13}C NMR results therefore complement the FTIR and ^{1}H NMR findings and provide additional evidence for the

formation of the desired imidazole derivatives. [16,17,18,19]

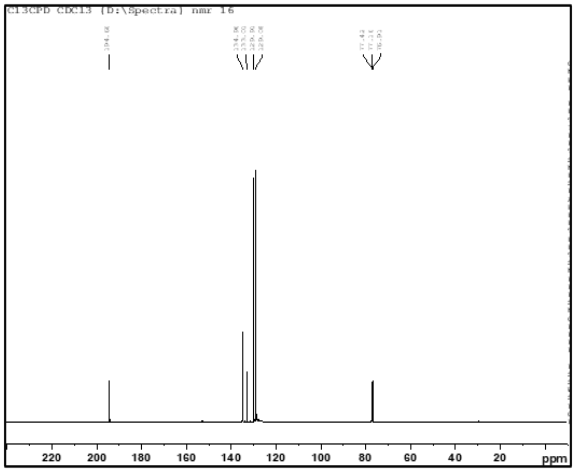

Figure 4. ^{13}C NMR spectrum of the synthesized imidazole derivative

3.8 Antibacterial Activity

The antibacterial activity of the synthesized imidazole derivatives was evaluated against *Staphylococcus aureus* at a concentration of 50 µg. Both selected derivatives exhibited measurable antibacterial activity under the experimental conditions. The cinnamaldehyde-derived imidazole produced an inhibition zone of approximately 2.0 mm, whereas the anisaldehyde-derived derivative showed an inhibition zone of approximately 1.8 mm.

Table 4. Antibacterial activity of **s**elected synthesized imidazole derivatives

Compound	Test organism	Concentration	Inhibition zone
Cinnamaldehyde-derived imidazole	*S. aureus*	50 µg	2.0 mm
Anisaldehyde-derived imidazole	*S. aureus*	50 µg	1.8 mm

The slightly higher inhibition observed for the cinnamaldehyde-derived derivative suggests that structural differences between the synthesized compounds may influence their antibacterial response. However, the inhibition zones were relatively small and the evaluation was limited to a single bacterial strain and concentration. Therefore, the present findings should be considered preliminary evidence of antibacterial activity**.** Further investigation involving multiple Gram-positive and Gram-negative bacterial strains, concentration-dependent studies, minimum inhibitory concentration (MIC) determination, suitable positive controls and statistical analysis would be necessary to establish the antibacterial potential of these compounds.

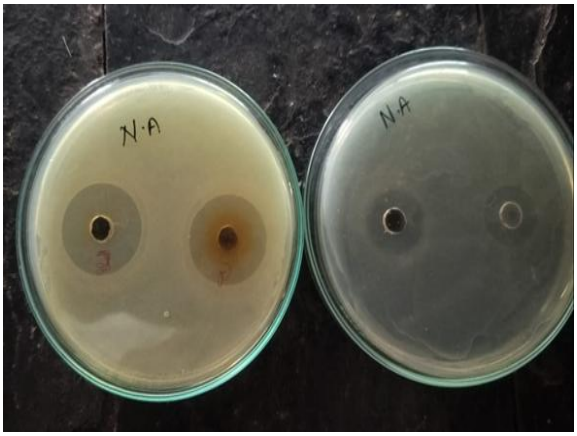

Figure 5. Antibacterial activity of the synthesized imidazole derivatives compared with reference antibiotics.

3.9 UV–Visible Investigation of Cu^{2+} Interaction

The interaction of the synthesized imidazole derivatives with Cu^{2+} ions was investigated using UV–Visible spectroscopy. A fixed concentration of the ligand solution was treated with increasing concentrations of $CuSO_4$ under buffered conditions, and the resulting spectral changes were monitored. A progressive change in absorption intensity was observed upon addition of Cu^{2+} ions, indicating an alteration in the electronic environment of the ligand following its interaction with the metal ion. The nitrogen atoms present within the imidazole framework can act as potential coordination sites for Cu^{2+}. Accordingly, the observed spectral changes may be associated with the formation of a ligand–Cu^{2+} coordination interaction or complex.

These results provide preliminary evidence for the ability of the synthesized imidazole derivatives to recognize and interact with Cu^{2+} ions. However, the present investigation does not establish a quantitatively validated sensing system. Parameters including the linear response range, limit of detection (LOD), limit of quantification (LOQ), binding or association constant, selectivity toward Cu^{2+} in the

presence of competing metal ions, response time and measurement reproducibility should be determined in future studies before describing the compounds as fully developed analytical Cu^{2+} sensors.

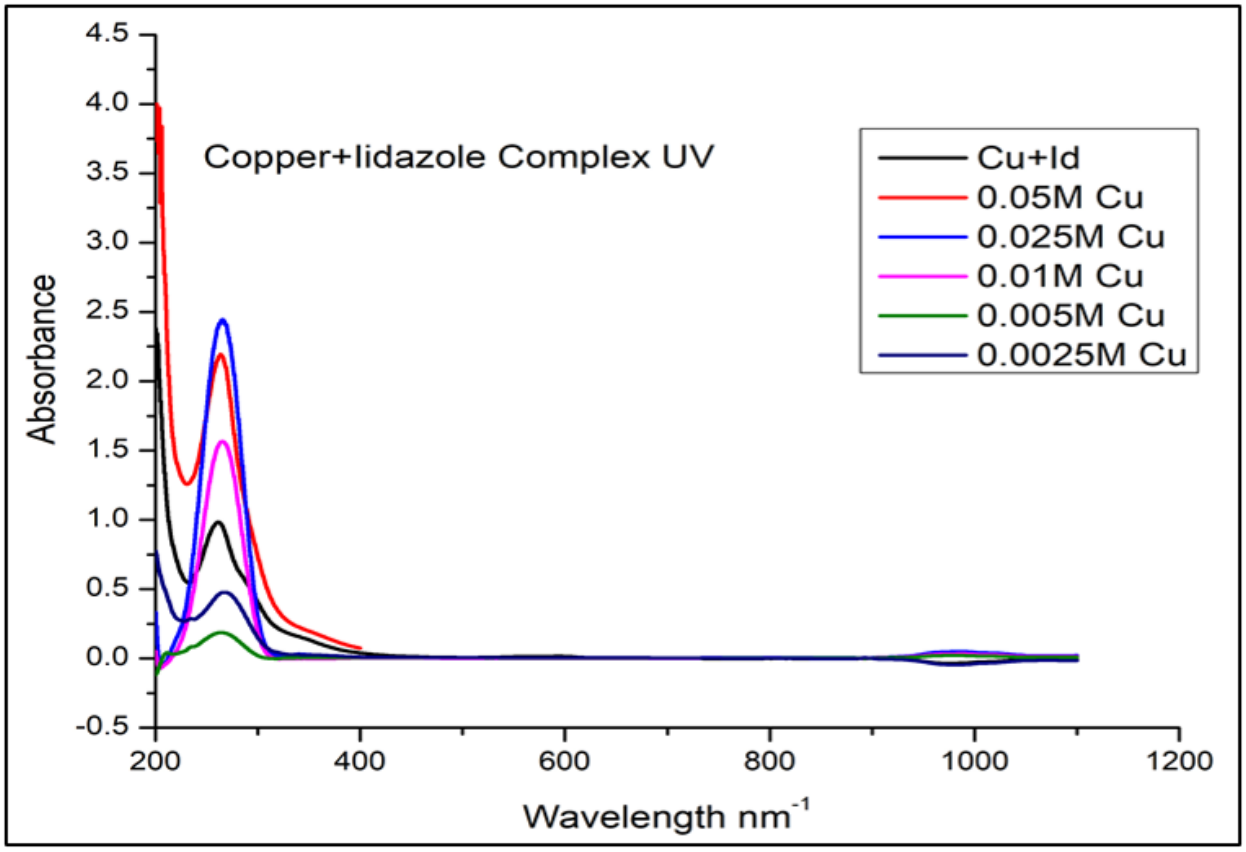

Figure 6. UV–Visible spectral changes observed during interaction of the synthesized imidazole derivative with Cu^{2+} ions.

3.10 Cyclic Voltammetry Investigation of Cu^{2+} Interaction

The interaction between the synthesized imidazole derivative and Cu^{2+} ions was further investigated by cyclic voltammetry. Electrochemical measurements were performed using a glassy carbon working electrode, platinum counter electrode and Ag/AgCl reference electrode in phosphate buffer at pH 7.0. The potential window was maintained between −0.2 and +0.8 V at a scan rate of 50 mV s^{-1}. Upon addition of the imidazole ligand to the Cu^{2+}-containing system, changes in both peak current and peak potential were observed. These electrochemical changes indicate a modification of the electrochemical environment of the copper species, which may arise from interaction or coordination between the ligand and Cu^{2+} ions.

At an addition volume of approximately 0.4 mL of the imidazole derivative, the formation of a visible precipitate was observed, accompanied by distortion of the voltammetric response. This behavior suggests a substantial interaction between the ligand and copper species under the experimental conditions. The appearance of a precipitate may also indicate the formation of a sparingly soluble copper–ligand complex. Taken together, the cyclic-voltammetric observations support the UV–Visible results and provide preliminary evidence for Cu^{2+} recognition by the synthesized imidazole derivatives. Nevertheless, because quantitative analytical parameters were not determined, the compounds should presently be described as potential Cu^{2+}-recognition ligands rather than fully validated electrochemical sensors. Further studies involving concentration-dependent electrochemical measurements, calibration curves, selectivity experiments, detection-limit calculations and reproducibility assessments are required to establish their analytical sensing performance.

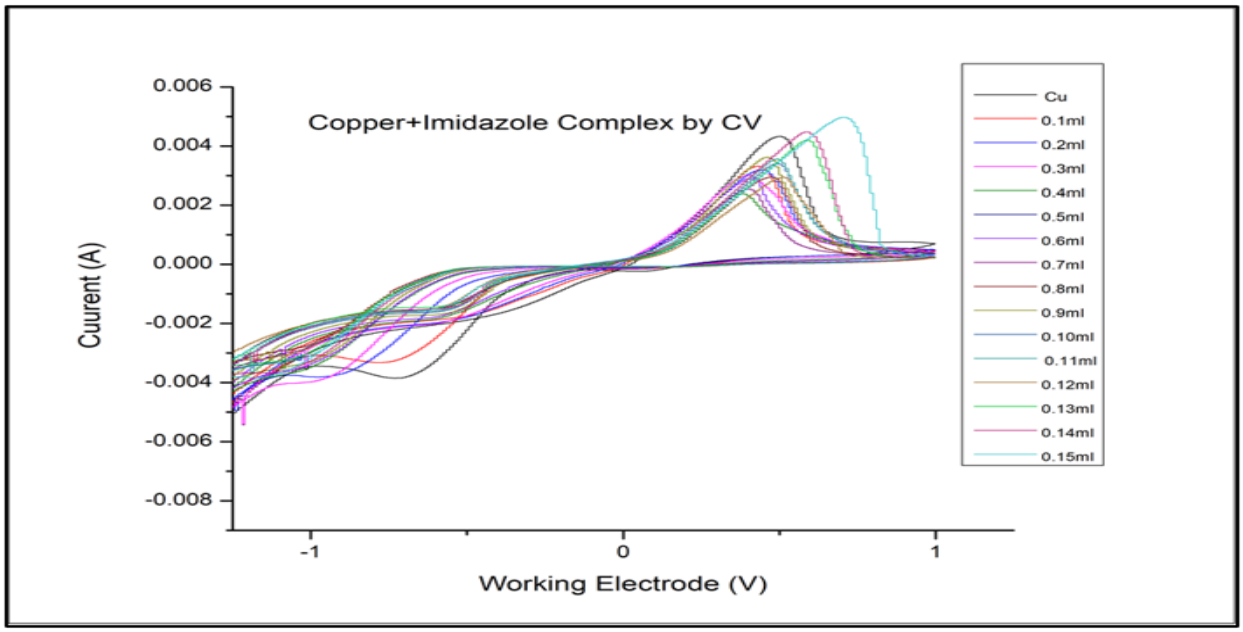

Figure 7. Cyclic voltammograms of the imidazole/Cu^{2+} system recorded at different ligand concentrations.

IV. CONCLUSION

A simple and environmentally preferable one-pot approach was developed for the synthesis of substituted imidazole derivatives using aqueous extracts of lemon, orange and pomegranate peels as naturally derived catalysts. Among the investigated catalytic systems, lemon peel extract exhibited the most favorable performance under solvent-free conditions, affording the cinnamaldehyde- and anisaldehyde-derived imidazole products in yields of 55.58% and 50.79%, respectively. The synthesized compounds were characterized using TLC, melting-point determination, UV–Visible spectroscopy, FTIR spectroscopy, ^{1}H NMR and ^{13}C NMR spectroscopy. The combined spectroscopic and analytical results were consistent with the formation of the proposed substituted imidazole frameworks. [10,11,12,13]

Preliminary biological evaluation demonstrated measurable antibacterial activity against *Staphylococcus aureus*, with the cinnamaldehyde-derived derivative showing a slightly greater inhibition zone than the anisaldehyde-derived derivative under the conditions investigated. In addition, UV–Visible and cyclic-voltammetric studies revealed distinct changes upon interaction with Cu^{2+} ions, suggesting that the synthesized imidazole derivatives possess potential Cu^{2+}-recognition capability. However, the antibacterial and Cu^{2+}-recognition studies were preliminary and do not, by themselves, establish therapeutic efficacy or a fully validated sensing platform. Further investigations involving broader microbial screening, MIC determination, concentration-dependent antibacterial studies, Cu^{2+} selectivity, calibration studies, detection limits, binding constants and reproducibility are necessary to establish these applications quantitatively.

Overall, the present study demonstrates a practical approach for converting fruit-peel waste into useful catalytic materials for the synthesis of functional imidazole derivatives. The combination of waste valorization, natural catalysis, solvent-free synthesis and preliminary biological and metal-ion recognition studies highlights the potential of this methodology as a sustainable route to value-added heterocyclic compounds.

ACKNOWLEDGEMENTS

The authors sincerely acknowledge the management, Principal and administration of Vidya Pratishthan's Arts, Science and Commerce College, Baramati, Maharashtra, for providing the laboratory facilities and institutional support required for this work. The authors also acknowledge the central analytical facilities for assistance with spectroscopic characterization and the Department of Microbiology

for support with the antibacterial studies. The authors express their sincere gratitude to colleagues and research associates who provided technical assistance during the experimental work.

CONFLICT OF INTEREST

The authors declare that they have no conflict of interest related to this work.

REFERENCES

[1] Debus H. Ueber die Einwirkung des Ammoniaks auf Glyoxal. Annalen der Chemie und Pharmacie. 1858;107:199–208.
[2] Radziszewski B. Zur Kenntniss der Imidazole. Chemische Berichte. 1882;15:1493–1496.
[3] Vogel AI. Vogel's Textbook of Practical Organic Chemistry. 5th ed. London: Longman Group; 1996.
[4] Furniss BS, Hannaford AJ, Smith PWG, Tatchell AR. Vogel's Textbook of Practical Organic Chemistry. 4th ed. London: Longman Scientific and Technical; 1989.
[5] Katritzky AR, Rees CW, Scriven EFV, editors. Comprehensive Heterocyclic Chemistry II. Oxford: Pergamon Press; 1996.
[6] Holla BS, Rao BS, Shridhara K, Akberali PM. Synthesis and antimicrobial activity of some novel imidazole derivatives. European Journal of Medicinal Chemistry. 2005;40:973–977.
[7] Kotharkar SA, Bhat AR, Khadse BG. Microwave-assisted synthesis of imidazole derivatives and their antimicrobial evaluation. International Journal of Pharmaceutical Sciences Review and Research. 2013;18(2):25–30.
[8] Zhang Y, Wang L, Li J. Microwave-assisted one-pot synthesis of substituted imidazoles under solvent-free conditions. RSC Advances. 2016;6:21412–21418.
[9] Zolfigol MA. Recent advances in solvent-free organic synthesis. Molecules. 2018;23:1683.
[10] Anastas PT, Warner JC. Green Chemistry: Theory and Practice. New York: Oxford University Press; 1998.
[11] Li CJ, Trost BM. Green chemistry for chemical synthesis. Proceedings of the National Academy of Sciences USA. 2008;105:13197–13202.
[12] Varma RS. Greener and sustainable chemistry: the role of solvent-free and microwave-assisted organic synthesis. Pure and Applied Chemistry. 2014;86(3):701–712.
[13] Sheldon RA. Green and sustainable manufacture of chemicals from biomass: state of the art. Green Chemistry. 2016;18:3180–3183.
[14] Silverstein RM, Webster FX, Kiemle DJ, Bryce DL. Spectrometric Identification of Organic Compounds. 8th ed. Hoboken: Wiley; 2014.
[15] Pavia DL, Lampman GM, Kriz GS, Vyvyan JR. Introduction to Spectroscopy. 5th ed. Boston: Cengage Learning; 2015.
[16] Keeler J. Understanding NMR Spectroscopy. 2nd ed. Chichester: Wiley; 2010.
[17] Günther H. NMR Spectroscopy: Basic Principles, Concepts and Applications in Chemistry. 3rd ed. Chichester: Wiley; 2013.
[18] Kemp W. Organic Spectroscopy. 3rd ed. London: Palgrave Macmillan; 1991.
[19] Claridge TDW. High-Resolution NMR Techniques in Organic Chemistry. 3rd ed. Oxford: Elsevier; 2016.
[20] Caswell DS, Spiro TG. Ultraviolet resonance Raman spectroscopy of imidazole, histidine, and $Cu(imidazole)_4^{2+}$. Journal of the American Chemical Society. 1986;108:6470–6477.
[21] Prenesti E, Berto S, Daniele PG. UV–Visible spectrophotometric characterization of copper(II) complexes with imidazole derivatives. Spectrochimica Acta Part A. 2003;59:201–207.
[22] Daniele PG, et al. Interaction of copper(II) with nitrogen-containing ligands: a spectroscopic study. Journal of Inorganic Biochemistry. 2002;88:37–43.
[23] Martins JG, Gameiro P, Barros MT, Soares HMVM. Potentiometric and UV–Visible studies of Cu(II)–imidazole complexes. Journal of Chemical & Engineering Data. 2010;55:3410–3417.
[24] Wu H, Kou F, Jia F, Liu B, Yuan J, Bai Y. Synthesis and characterization of benzimidazole copper(II) complex: DNA binding and antioxidant activity. Bioinorganic Chemistry and Applications. 2011;2011:105431.
[25] Mullaivendhan J, et al. Cu(II)-catalysed synthesis of imidazole derivatives and spectroscopic characterization. BMC Chemistry. 2023;17:155.

[26] Finšgar M, Xhanari K. Electrochemical and surface analysis of 2-phenylimidazole adsorbed on copper. Coatings. 2018.